Coherent surface phonon dynamics at K-covered Pt(111) surfaces investigated by time-resolved second harmonic generation

Masanori Fuyuki, Kazuya Watanabe, and Yoshiyasu Matsumoto*
Department of Photoscience, The Graduate University for Advanced Studies (SOKENDAI), Hayama, Kanagawa 240-0193, Japan and Institute for Molecular Science, Okazaki, Aichi 444-8585, Japan
(Received 29 July 2006; published 13 November 2006)

We have investigated coherently excited surface phonons at K-covered Pt(111) surfaces by using femtosecond time-resolved second harmonic generation spectroscopy. The frequency of the K-Pt stretching phonon mode depends on the superstructure of K: 5.0–5.3 and 4.5–4.8 THz for (2×2) and $(\sqrt{3}\times\sqrt{3})R30°$ superstructures, respectively. In addition to the stretching mode, three surface phonon modes are simultaneously observed when the $(\sqrt{3}\times\sqrt{3})R30°$ superstructure is formed. The decay time of the K-Pt stretching mode becomes shorter and its frequency redshifts as the absorbed fluence of the pump pulse increases. This is in stark contrast to the Pt surface phonon modes whose frequencies are independent of fluence. The fluence dependence of the K-Pt stretching mode is interpreted to be due to anharmonic coupling between the K-Pt stretching and lateral modes.

DOI: 10.1103/PhysRevB.74.195412 PACS number(s): 78.47.+p, 68.35.Ja, 68.43.Pq, 82.53.St

I. INTRODUCTION

Because of the dense electronic states of metals, many of their physical properties are determined by nonadiabatic couplings between electrons and phonons. Properties and dynamics of adsorbates on metal surfaces are no exception. Since nuclear motions of adsorbates strongly couple to electron motions in metals by electron-hole pair creation, strong nonadiabaticity is essential in various processes on metal surfaces. In particular, the effects of nonadiabatic coupling have been more clearly brought to light by studies on adsorbate vibrational damping and pure dephasing,[1–3] desorption induced by multiple electronic transitions (DIMETs),[4] frustrated photodesorption of alkali-metal atoms from noble metals,[5,6] and femtochemistry on metal surfaces.[7–9] For a deeper understanding of nonadiabatic couplings at metal surfaces, it is vital to observe nuclear motions under electronic excitation directly in the time domain. However, these measurements are still very rare.

Alkali-metal atoms on metal surfaces provide an interesting opportunity for investigation of nonadiabatic couplings. Since alkali-metal adsorption systems are some of the simplest chemisorption systems, their geometric[10] and electronic structures[11] have been extensively studied. Electronic interactions between alkali-metal adsorbates and metal surfaces strongly depend on coverage. A delicate balance between adsorbate-adsorbate and adsorbate-metal interactions gives rise to various ordered structures of alkali-metal adsorbates. These rich pieces of information make these adsorption systems very suitable to explore nonadiabatic couplings at metal surfaces as a function of coverage.

A laser pulse with a duration shorter than the oscillation frequencies of surface phonons can create coherent surface phonons, i.e., a lattice mode with a large number of phonons in one mode with a constant phase-lattice relation.[12] Recently we have demonstrated the time-domain observation of coherent surface phonons on Cs-covered Pt(111) surfaces by time-resolved second harmonic generation (TRSHG) spectroscopy.[13–16] In this method, surface phonons are excited coherently by irradiation of an ultrashort pump laser pulse and the evolution of coherent surface phonons is probed by intensity modulations of the second harmonic (SH) of probe pulses as a function of pump-probe delay.[17] Since the ultrashort pump pulse also creates nonequilibrium conditions in which the electron temperature of the metal is substantially higher than the lattice temperature, this pump-probe spectroscopy is very suitable to study the role of nonadiabatic coupling in excitation, vibrational damping, and pure dephasing processes.[14] This situation is very different from the traditional energy-domain techniques such as high-resolution electron energy loss spectroscopy (HREELS) and inelastic He atom scattering (HAS); although energy loss in these spectroscopic methods is associated with nonadiabatic processes, metal surfaces are usually nearly in thermal equilibrium during scattering events.

In the previous reports on Cs-covered Pt(111) surfaces,[13–16] we have identified coherent nuclear motions of Cs-Pt stretching and Pt-substrate Rayleigh phonon modes by TRSHG as a function of Cs coverage. The coverage dependence of the initial amplitude of the Cs-Pt coherent stretching mode suggests that the resonant excitation between Cs-induced states in a Cs metallic quantum well plays an important role in creating vibrational coherence.[15] Moreover, the fast-decaying component of the Cs-Pt stretching mode grows as the pump fluence increases. This is interpreted in terms of pure dephasing caused by anharmonic coupling with low-frequency lateral modes of Cs.[14] However, Cs/Pt(111) has been the only alkali-metal adsorption system studied so far by this method. Obviously more examples are needed to answer important questions on excitation mechanisms, coherent phonon dynamics, and nonadiabatic coupling. Thus, we have started a systematic study on various combinations of alkali metals with metal substrates.

This paper describes the coherent surface phonon dynamics on potassium-covered Pt(111) surfaces investigated by TRSHG. We focus on higher coverages of the alkali metal in which the alkali-metal adlayer forms a metallic quantum well.[18] In this condition, surface phonons are expected to couple strongly to an adsorbate-induced surface electronic state near the Fermi level. In contrast to Cs/Pt(111) where

the frequency of the Cs-Pt stretching mode is very close to the Rayleigh mode of Pt(111),[15] the adsorption system of K/Pt(111) allows us to observe substrate surface phonon modes more clearly, since the frequency of the K-Pt stretching mode is much higher than those of the substrate surface phonon modes.

II. EXPERIMENT

The experiments were carried out in an ultrahigh-vacuum (UHV) chamber equipped with a cylindrical mirror analyzer (Vacuum General, VG100AX) for Auger electron spectroscopy (AES). A Pt(111) surface was cleaned by repeated cycles of sputtering, annealing, and oxygen treatment. Potassium atoms from a well-degassed alkali-metal dispenser (SAES Getters) were deposited on the clean Pt(111) surface at 110 K. The potassium coverage θ on Pt(111) was calibrated by measuring the Auger peak intensity ratios of K(243 eV) to Pt(65 eV) as a function of K deposition time t_K.

The procedures for TRSHG measurements are basically the same as reported previously.[13–15] Briefly, second harmonic outputs of near-infrared ($\lambda=800$ nm) laser pulses (duration=130 fs) from a Ti:sapphire regenerative amplifier (Spectra Physics, Spitfire, 1 kHz) pumped two sets of a home-built noncollinear optical parametric amplifier (NOPA). The NOPA systems supplied ultrashort pulses independently tunable from 2.0 to 2.5 eV, which were used as pump and probe pulses. A typical NOPA output energy was ~ 4 μJ per pulse right after the BBO (β-BaB_2O_4)crystal in the NOPA system. Both pump and probe pulses were p polarized and their photon energies were fixed at 2.14 eV. The adjustable group velocity dispersion was introduced by quartz prism pairs for pulse compression. Pump and probe pulses were focused on the sample in the UHV chamber at an incident angle of $\sim 68°$. The pulse duration of pump and probe pulses was estimated to be 25 fs by monitoring sum-frequency signals of pump and probe pulses from the sample surface. The SH intensity of a probe pulse was detected by a photomultiplier tube as a function of pump-probe delay t. An optical chopper was inserted in the optical path of the pump pulse for detection of pump-induced SH intensity modulations. In this paper, transient changes of SH intensity ΔI_{SH} are defined as $\Delta I_{SH}(t)=[I_{SH}(t)-I^0_{SH}]/I^0_{SH}$, where $I_{SH}(t)$ and I^0_{SH} are SH intensities with and without pump pulses, respectively. Each data point of TRSHG traces was obtained by averaging signals for 3000 laser shots.

III. RESULTS AND DISCUSSION

A. Calibration of K coverage

Figure 1(a) shows Auger peak intensity ratios of K(243 eV) to Pt(65 eV) as a function of t_K. These data can be expressed by two curves with a break at $t_K=100$ s under the assumption of layer-by-layer growth. The break point appeared as a result of the second-layer growth.[19] Pirug and Bonzel[20] investigated adsorption structures of K on Pt(111) by low-energy electron diffraction (LEED), x-ray photoelectron spectroscopy, and AES. They concluded that the second layer starts to grow at $\theta=0.38$ monolayer (ML) (1 ML=1.5×10^{15} atoms/cm^2). Therefore, we determined the K coverage at $t_K=100$ s to be 0.38 ML and all K coverages described in this paper are referenced to this value.

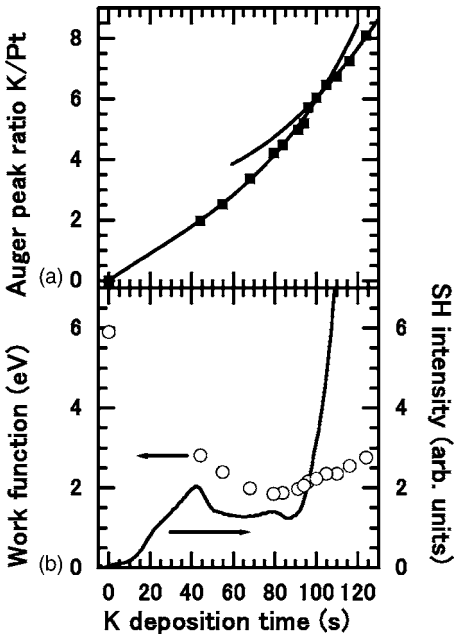

FIG. 1. (a) Auger peak ratio of K(243 eV) to Pt(65 eV) as a function of K deposition time. The solid lines are drawn as a guide to the eyes. (b) Work function (open circles) and SHG intensity (solid lines) of p-polarized pulses ($\lambda=800$ nm) from a Pt(111) surface as a function of K deposition time.

Figure 1(b) shows work functions and SH intensities of p-polarized laser pulses ($\lambda=800$ nm) from the surface vs t_K. The SH intensity increases almost linearly with t_K up to $t_K\sim40$ s, decreases slightly, and is strongly enhanced over $t_K\sim90$ s. Since these characteristic features of SH intensities are useful for monitoring the growth of a K adlayer during deposition, we routinely monitored SH intensities in each run.

B. Coverage dependence

When a surface phonon mode is coherently excited by a pump pulse, nonstationary coherent nuclear motions modulate electronic degrees of freedom. Thus, the second-order optical susceptibility $\chi^{(2)}(2\omega)$ and hence macroscopic polarization $P^{(2)}(2\omega)$ are modulated by the coherent motions. Since this modulation is small, $\chi^{(2)}$ can be expanded at the equilibrium position of a nuclear coordinate $Q=Q_0$ relevant to the coherent oscillation in terms of nuclei displacement δQ as

$$\chi^{(2)} = \chi^{(2)}|_{Q=Q_0} + \left.\frac{\partial\chi^{(2)}}{\partial Q}\right|_{Q=Q_0}\delta Q + \cdots . \qquad (1)$$

Because SH intensity is proportional to $|\chi^{(2)}|^2$, the leading term of the modulation due to the coherent oscillation is the cross term between the first and second terms in Eq. (1). Thus, the time evolution of the coherent oscillation can be

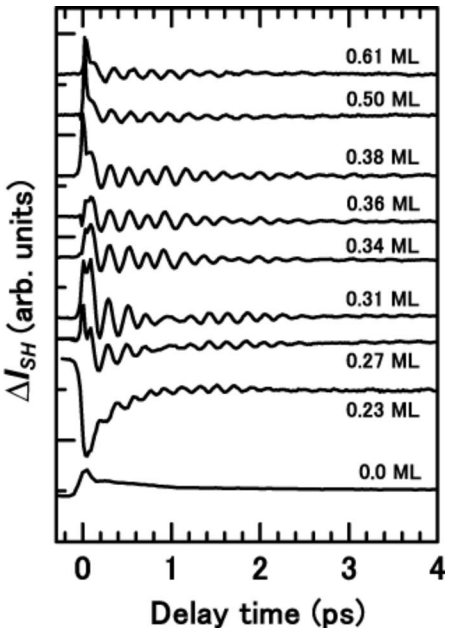

FIG. 2. TRSHG traces taken from K-covered Pt(111) surfaces at various θ. The absorbed fluence of the pump pulse is 0.4 mJ/cm^2 per pulse.

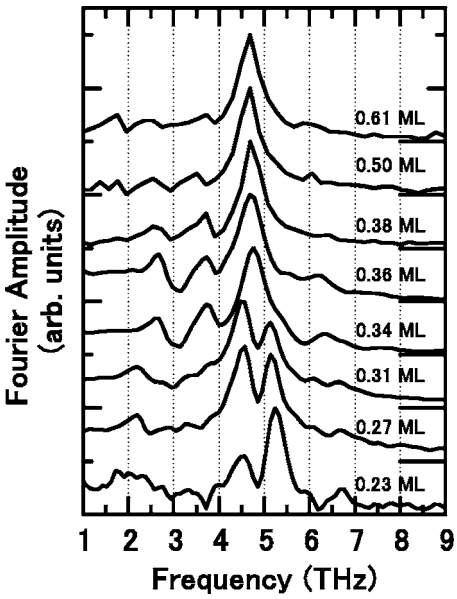

FIG. 3. Fourier-transformed spectra of the oscillatory components in the TRSHG traces in Fig. 2. The spectra are normalized at their peak intensities.

detected by measuring ΔI_{SH} of a probe pulse as a function of t.[15]

Figure 2 shows TRSHG traces taken from K-covered Pt(111) surfaces as a function of θ. The TRSHG trace from the clean Pt(111) surface shows fast and slowly decaying components without any periodic oscillating modulations. Since the decay behavior resembles the temporal variations of electron temperature predicted by numerical integration of coupled diffusion equations,[21,22] the TRSHG signals are likely attributed to hot electrons created by substrate photon absorption.[15] In contrast, the TRSHG traces from K-covered Pt(111) surfaces show oscillatory components clearly. Figure 3 shows the Fourier-transformed (FT) spectra of the oscillatory parts in the TRSHG traces in Fig. 2. We used the oscillatory parts of TRSHG traces in $t \geqslant 60$ fs after subtracting background components whose frequencies are less than 1 THz. The TRSHG traces were decomposed into oscillating and background components by linear prediction singular-value decomposition (LPSVD) based on the procedure described elsewhere.[15,23,24] Parameters obtained in the LPSVD analysis are listed in Table I. Typical uncertainties are ±2% for frequency, ±8% for initial phase, and ±10% for decay time. Here, both vibrational damping and pure dephasing contribute to the decay time. These uncertainties were estimated by the statistical distributions of the fitted parameters obtained in the different sets of data.

The FT spectra in Fig. 3 show two prominent peaks at 4.5 and 5.2 THz below θ=0.31 ML. At θ=0.23 ML, the peak at 5.2 THz is stronger than that at 4.5 THz, but the latter peak dominates over the former with increase of θ. The HREELS study by Klünker *et al.*[25] reported that a single loss peak due to the K-Pt stretching mode shifts from 5.3 to 4.7 THz as θ increases from 0.16 to 0.33 ML. The two peaks observed in the TRSHG measurements and their intensity alternation with θ are consistent with the HREELS result, although the HREELS spectrum shows only a broad peak around 5 THz owing to its poor resolution and the relatively high surface temperature. Therefore, the two oscillating components observed in the TRSHG measurements are attributed to the coherent K-Pt stretching motions on Pt(111).

The problem is why there are two frequency components for the K-Pt stretching mode. Potassium adlayers are known to form two ordered structures on Pt(111). According to the LEED study,[20] while a (2×2) structure is formed at $0.20 \leqslant \theta \leqslant 0.25$ ML, this structure is mixed with a $(\sqrt{3}\times\sqrt{3})R30°$ structure and eventually the K adlayer entirely turns into the $(\sqrt{3}\times\sqrt{3})R30°$ structure at θ=0.33 ML. The alternation in the intensities of the peaks at 4.5 and 5.2 THz as a function of θ is qualitatively correlated with the change in the superstructure of K adlayers. Thus, we assign the peaks at 5.2 and 4.5 THz for $0.23 \leqslant \theta \leqslant 0.31$ ML to the K-Pt stretching modes of (2×2) and $(\sqrt{3}\times\sqrt{3})R30°$ domains, respectively.

At θ=0.34 ML the FT spectrum shows significantly different features from those in $\theta \leqslant 0.31$ ML. First, the two peaks observed at $\theta \leqslant 0.31$ ML apparently merge into one peak at 4.7 THz. As stated earlier, since the $(\sqrt{3}\times\sqrt{3})R30°$ structure is completed at θ=0.33 ML,[20] (2×2) domains and hence the 5.2 THz peak of (2×2) domains disappears. Thus, the change in the FT spectra implies that the frequency of the K-Pt stretching mode in the $(\sqrt{3}\times\sqrt{3})R30°$ structure shifts from 4.5 THz at $\theta \leqslant 0.31$ ML to 4.7 THz at θ=0.34 ML. This might indicate that the frequency shift is associated with the increase in the domain size of the superstructure at θ=0.34 ML. If so, the peak originating in the $(\sqrt{3}\times\sqrt{3})R30°$ structure would shift as the coverage increases from θ=0.23 to 0.31 ML. However, the peak does not shift gradually in the coverage range but suddenly shifts to 4.7 THz at θ=0.34 ML. At this moment, the origin of the

TABLE I. Parameters obtained from the LPSVD analysis of TRSHG signals. $\omega/2\pi$ is frequency, τ is decay time, ϕ is initial phase, and A is relative amplitude normalized at the largest amplitude for each coverage.

θ (ML)	$\omega/2\pi$ (THz)	τ (ps)	ϕ (deg)	A
0.23	5.25	1.62	17	2.44
	4.58	1.64	37	1.00
0.27	5.08	0.95	−123	0.75
	4.60	0.79	−151	1.00
	2.25	0.93	−98	0.22
0.31	5.09	0.89	−154	0.74
	4.55	0.92	−148	1.00
	2.21	0.68	−75	0.28
0.34	5.57	0.76	13	0.12
	4.75	0.82	−156	1.00
	3.79	1.32	−130	0.21
	3.27	1.13	71	0.10
	2.71	1.43	−141	0.16
0.36	4.71	0.96	−164	1.00
	3.78	1.75	−151	0.16
	3.27	1.34	32	0.12
	2.69	2.41	−136	0.14
0.38	4.72	1.10	−167	1.00
	3.88	2.27	−212	0.14
	3.43	0.47	−29	0.25
	2.69	3.33	−121	0.11
0.50	4.64	1.03	−152	1.00
	3.53	2.68	−127	0.08
	2.69	3.42	−107	0.06
0.61	4.65	0.96	−156	1.00
	3.76	2.67	−134	0.07
	2.51	1.42	−57	0.12

sudden shift is not clear. The frequency of the K-Pt stretching mode stays almost constant for $0.34 \leqslant \theta \leqslant 0.38$ ML, then slightly shifts from 4.7 to 4.6 THz at $0.38 \leqslant \theta \leqslant 0.61$ ML. This may be due to adsorption of K atoms in the second layer.

While the oscillation frequency and decay time do not change with increasing coverage above $\theta=0.38$ ML, the oscillation amplitude decreases. Since an electronic transition from the alkali-metal-induced occupied state to an image potential state resonantly enhances the modulation amplitudes in TRSHG traces,[26] the changes in the electronic structure with increase of θ may manifest in a decrease of oscillation amplitude. Another possibility is due to the decrease in the surface area of the first-layer adsorbates without alkali-metal atoms in the second layer. When alkali-metal atoms adsorb in the second layer, the K-Pt stretching mode is perturbed and its frequency could be greatly shifted. Since no appreciable frequency components were observed in the FT spectra other than that of the K-Pt stretching mode in the first layer, the first-layer alkali-metal atoms with second-layer atoms may not be excited coherently.

Another salient feature in the FT spectrum at $\theta=0.34$ ML is that the peaks at 2.7, 3.4, and 3.8 THz appear. The appearance of these peaks is also related to the completion of $(\sqrt{3}\times\sqrt{3})R30°$ superstructure at this coverage. Because of this superstructure, the surface Brillouin zone of a clean Pt(111) surface is reduced such that the zone boundary at the $\bar{K}$ point is folded back to the $\bar{\Gamma}$ point. This makes it possible to observe surface phonon modes of Pt(111) by optical spectroscopy such as TRSHG.

Kern *et al.*[27] and Bortolani *et al.*[28] investigated phonon modes at a clean Pt(111) surface by inelastic HAS. Phonon dispersion data were analyzed by surface lattice dynamics simulations with a slab of N equally spaced atomic planes. From the best-fit results the observed inelastic scattering data along the $\bar{\Gamma}$-$\bar{K}$ direction are well described by three surface phonon modes: Rayleigh, pseudo-Rayleigh, and longitudinal resonance modes. At the $\bar{K}$ point, the lattice dynamics simulations with modified nearest-neighbor force constants at the surface provide the frequency and normal coordinate of each surface phonon. The Rayleigh and longitudinal resonance modes merge into the same frequency of 11 meV (2.7 THz) at the $\bar{K}$ point. The pseudo-Rayleigh phonon mode is located at 14 meV (3.4 THz). The normal mode analysis indicates that only the Rayleigh mode shows substantial displacements of atoms in the second plane as well as the first plane of the Pt surface at $\bar{K}$, but atom displacements of the other two modes are mostly limited in the first plane.[28] In addition to these modes, Kern *et al.*[27] reported an additional mode at ~16 meV (3.8 THz) at $\bar{K}$ at temperatures much higher than 350 K. This was assigned to the mode polarized longitudinally to the surface in the Pt first layer and polarized vertically with a larger amplitude in the Pt second layer. However, this assignment was later questioned, since inelastic HAS is not sensitive to the motions in the second layer.[28]

Recently, Chis *et al.*[29] conducted a first-principles calculation of the phonons of Cu(111). They showed that hybridization takes place between a longitudinal resonance mode in the first layer and a second-layer shear-vertical mode with a large vertical displacement near the $\bar{M}$ point. Since a large fluctuation of the electron density at the turning point of a He atom is expected due to the hybridized mode, this calculation suggests that the second-layer shear-vertical displacements may be detected by HAS measurements.

Although the ambiguity remains in the assignments of the substrate surface phonon modes, the frequencies observed in the TRSHG measurements are in reasonable agreement with those reported in the HAS measurements. Therefore, we tentatively assigned the modes at 2.7, 3.4, and 3.8 THz to the mixture of the Rayleigh and the longitudinal resonance modes, the pseudo-Rayleigh phonon mode, and the mode mainly localized in the second layer, respectively. The mutual agreement between the inelastic HAS performed for a clean Pt(111) surface and TRSHG measurements done for K-covered Pt(111) surfaces in the current study suggests that the surface phonon modes of Pt(111) are not significantly affected by K adsorption. This is consistent with LEED structural analysis and density functional theory calculations performed for K/Pt(111) by Moré *et al.*[30] They showed that

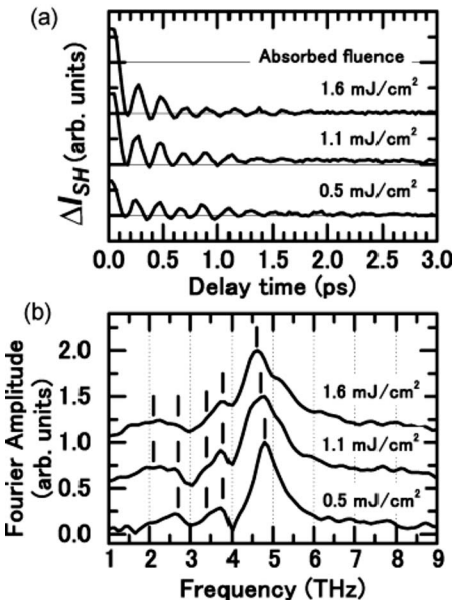

FIG. 4. (a) TRSHG traces taken from 0.38 ML K-covered Pt(111) surfaces as a function of the laser fluence of a *p*-polarized pump pulse ($h\nu$=2.14 eV) absorbed by the Pt substrate. (b) Fourier-transformed spectra of the oscillatory components in the TRSHG traces.

K atoms adsorbed at threefold hcp sites forming the $(\sqrt{3}\times\sqrt{3})R30°$ structure induce very small spatial distortions near the surface, i.e., less than 1.0%. Therefore, although many alkali-atom adsorption systems on metal surfaces are reported to show significant rumpling and even reconstruction of the surfaces,[10] the K adsorption does not affect the Pt surface phonon modes significantly.

As stated earlier, the frequency of the K-Pt stretching mode depends on θ. In addition, the decay characteristics also change with θ as shown in Table I. The decay time of the K-Pt stretching mode in the (2×2) structure at ~5.2 THz becomes shorter as θ increases from 0.23 to 0.31 ML, whereas that in the $(\sqrt{3}\times\sqrt{3})R30°$ structure at ~4.5 THz becomes longer as θ changes from 0.27 to 0.38 ML. In these coverage regions, the dominant K superstructure changes from (2×2) to $(\sqrt{3}\times\sqrt{3})R30°$ with the increase of coverage. This transition of the superstructure decreases the average domain size of (2×2), while it increases that of $(\sqrt{3}\times\sqrt{3})R30°$. Thus, the coverage dependence of decay times suggests that the domain size of the K superstructure affects the decay time of the K-Pt stretching mode: the larger domain sizes grow, the longer decay times become.

C. Pump fluence dependence

Resonant impulsive stimulated Raman excitation can be a plausible excitation mechanism of the coherent surface phonons observed in this study. We found that the amplitude of K-Pt stretching coherent phonon signals is resonantly enhanced by the electronic transition from the alkali-metal-induced occupied state to an image potential state.[26] In addition to the resonant transition, photons are absorbed in the bulk platinum to create electron-hole pairs. As a result, the electron temperature increases in a short period of time. With a typical photon fluence used in the current study, 0.4 mJ/cm^2, a two-temperature model[21,22] indicates that the electron temperature of the substrate rapidly reaches 1000 K at $t\sim30$ fs and decays with a time constant of ~1 ps after the pump pulse irradiation. Since the decay time of the coherent K-Pt stretching mode is in the range of 1–2 ps, the coherent oscillation dephases while electron temperature is substantially higher than the lattice temperature.

Figures 4(a) and 4(b) show the pump power dependence of TRSHG traces and their FT spectra, respectively, taken from the 0.38 ML K-covered Pt(111) surface. The following points are noteworthy. As absorbed fluence increases, the peak due to the K-Pt stretching mode shows clear redshifts and broadenings. When the absorbed fluence is changed from 0.5 to 1.6 mJ/cm^2, the peak frequency shifts from 4.8 to 4.6 THz, while the decay time changes from 0.78 ± 0.02 to 0.47 ± 0.07 ps. These changes can be accounted for by the anharmonic couplings with lateral modes of K. If the K-Pt stretching mode couples to the lateral modes, the stretching frequency is modulated by the anharmonic couplings. This results in pure dephasing of the coherently excited K-Pt stretching mode.[14]

Excitation of lateral modes can be realized in the following ways. One possibility is that hot electrons produced by a pump pulse are resonantly scattered with alkali-metal adsorbates, resulting in excitation of the lateral modes. As fluence increases, multiple inelastic scattering populates the higher vibrational states of lateral modes[31] as in the case of DIMET. The similar trend was observed in the Cs/Pt(111) measurements.[14] However, one difference exists in decay dynamics between the two systems. For the absorption fluence below 0.3 mJ/cm^2 (with a pulse duration of 25 fs), the decay time of K-Pt stretching mode is τ=1.1 ps and independent of pump fluence. For an absorption fluence of 1.1 mJ/cm^2 leading to a maximum electronic temperature of 1600 K, the decay time is reduced to τ=0.45 ps. The decay rate increases by a factor of 2.5. In the case of the Cs-Pt stretching mode, the decay time is 1.9 ps and independent of the pump fluence below 1.0 mJ/cm^2 (with a pulse duration of 130 fs). For an absorption fluence of 1.7 mJ/cm^2 leading to a maximum electronic temperature of 1500 K, which is almost equivalent to the case of K/Pt(111) with a fluence of 1.1 mJ/cm^2; the decay time is still 1.9 ps.[14] The decay time scarcely increases. This marked difference in decay characteristics suggests that the anharmonic coupling between the stretching and lateral modes of K-Pt is significantly larger than that of Cs-Pt.

The other possibility is that lateral modes can be excited coherently. Note that a broad peak at ~2 THz becomes appreciable with the increase of absorbed fluence. Since the surface phonon mode with the lowest frequency is the Rayleigh mode of 2.7 THz at the $\bar{K}$ point, this peak cannot be assigned to substrate surface phonons. A number of alkali-metal adatom vibrational energies are compiled by Finberg *et al.*[32] The frequencies of both stretching and lateral modes scale approximately with the inverse square root of alkali-metal masses and the frequencies of lateral modes roughly fall in the range of 20–30 % of those of stretching modes.

Therefore, the peak at ~2 THz could be assigned to a lateral mode of K adatoms.

In contrast to the K-Pt stretching mode, the peaks in the FT spectra due to the other surface phonon modes of the Pt substrate show little shifts as the absorbed fluence of a pump pulse increases. This indicates that the anharmonicity of a surface phonon of the Pt substrate is much smaller than that of the K-Pt stretching mode, so that the surface phonon frequency is insensitive to hot electrons created by a pump pulse. If one considers that the melting point of Pt is much higher than the desorption temperature of K adsorbates from Pt(111), it is naturally understandable that the anharmonicity of the K-Pt stretching mode is significantly larger than those of the substrate surface phonon modes.

IV. CONCLUSION

We have observed K-adsorbate-induced phonon modes as well as Pt substrate surface phonon modes coherently excited by ultrashort laser pulses at the K-covered Pt(111) surface by TRSHG. As transient electron temperature increases with absorbed pump fluence, they behave differently. The K-Pt stretching mode shows a large anharmonicity via coupling to lateral modes. In contrast, the substrate surface phonon modes do not show any indications of anharmonicity within the laser fluence used in the current study.

ACKNOWLEDGMENTS

This work was supported in part by Grants-in-Aid for Scientific Research (S) (Grant No. 17105001) from Japan Society for the Promotion of Science (JSPS) and Scientific Research on Priority Area (417 Fundamental Science and Technology of Photofunctional Interfaces, and 432 Molecular Nano Dynamics) from the Ministry of Education, Culture, Sports, Science and Technology (MEXT) of Japan.

*Electronic address: matsumoto@ims.ac.jp

[1] Y. J. Chabal, Surf. Sci. Rep. **8**, 211 (1988).
[2] H. Ueba, Prog. Surf. Sci. **55**, 115 (1997).
[3] Y. Matsumoto and K. Watanabe, Chem. Rev. (Washington, D.C.) **106**, 4234 (2006).
[4] J. A. Misewich, T. F. Heinz, P. Weigand, and A. Kalamarides, *Laser Spectroscopy and Photochemistry on Metal Surfaces* (World Scientific Publishing, Singapore, 1995), Chap. 19, pp. 764–826.
[5] H. Petek, M. J. Weida, H. Nagano, and S. Ogawa, Science **288**, 1402 (2000).
[6] H. Petek and S. Ogawa, Annu. Rev. Phys. Chem. **53**, 507 (2002).
[7] M. Bonn, S. Funk, C. Hess, D. N. Denzler, C. Stempfl, M. Scheffler, M. Wolf, and G. Ertl, Science **285**, 1042 (1999).
[8] D. N. Denzler, C. Frischkorn, C. Hess, M. Wolf, and G. Ertl, Phys. Rev. Lett. **91**, 226102 (2003).
[9] C. Frischkorn and M. Wolf, Chem. Rev. (Washington, D.C.) **106**, 4207 (2006).
[10] R. D. Diehl and R. McGrath, Surf. Sci. Rep. **23**, 43 (1996).
[11] S.-Å. Lindgren and L. Walldén, *Some Properties of Metal Overlayers on Metal Substrates*, Handbook of Surface Science Vol. 2 (Elsevier, Amsterdam, 2000), Chap. 13, pp. 899–951.
[12] T. Dekorsy, G. C. Cho, and H. Kurz, *Coherent Phonons in Condensed Media*, Topics in Applied Physics Vol. 76 (Springer-Verlag, Berlin, 2000), Chap. 4, pp. 169–209.
[13] K. Watanabe, N. Takagi, and Y. Matsumoto, Chem. Phys. Lett. **366**, 606 (2002).
[14] K. Watanabe, N. Takagi, and Y. Matsumoto, Phys. Rev. Lett. **92**, 057401 (2004).
[15] K. Watanabe, N. Takagi, and Y. Matsumoto, Phys. Rev. B **71**, 085414 (2005).
[16] K. Watanabe, N. Takagi, and Y. Matsumoto, Phys. Chem. Chem. Phys. **7**, 2697 (2005).
[17] Y.-M. Chang, L. Xu, and H. K. Tom, Chem. Phys. **251**, 283 (2000).
[18] J. M. Carlsson and B. Hellsing, Phys. Rev. B **61**, 13973 (2000).
[19] E. L. Garfunkel and G. A. Somorjai, Surf. Sci. **115**, 441 (1982).
[20] G. Pirug and H. P. Bonzel, Surf. Sci. **194**, 159 (1988).
[21] M. I. Kaganov, I. M. Lifshitz, and L. V. Tanatarov, Sov. Phys. JETP **31**, 232 (1957).
[22] S. I. Anisimov, B. L. Kapeliovich, and T. L. Perel'man, Sov. Phys. JETP **39**, 375 (1974).
[23] H. Barkhuijsen, R. de Beer, W. M. M. J. Boveé, and D. V. Ormondt, J. Magn. Reson. (1969-1992) **61**, 465 (1985).
[24] A. E. Johnson and A. B. Myers, J. Chem. Phys. **104**, 2497 (1996).
[25] C. Klünker, C. Steimer, J. B. Hannon, M. Giesen, and H. Ibach, Surf. Sci. **420**, 25 (1999).
[26] M. Fuyuki (unpublished).
[27] K. Kern, R. David, R. L. Palmer, G. Comsa, and T. S. Rahman, Phys. Rev. B **33**, 4334 (1986).
[28] V. Bortolani, A. Franchini, G. Santoro, J. P. Toennies, C. Wöll, and G. Zhang, Phys. Rev. B **40**, 3524 (1989).
[29] V. Chis, Ph.D. thesis, Göteborg University, 2006.
[30] S. Moré, W. Berndt, A. M. Bradshaw, and R. Stumpf, Phys. Rev. B **57**, 9246 (1998).
[31] F. Fournier, W. Zheng, S. Carrez, H. Dubost, and B. Bourguignon, J. Chem. Phys. **121**, 4839 (2004).
[32] S. E. Finberg, J. V. Lakin, and R. D. Diehl, Surf. Sci. **496**, 10 (2002).